Characterization of EMF hotspots for realistic exposure assessment in end-to-end simulations using a hybrid QuaDRiGa/FDTD tool

Robin Wydaeghe[1, 2], Sergei Shikhantsov[1, 2], Emmeric Tanghe[1, 2], Günter Vermeeren[1, 2], and Wout Joseph[1, 2]
[1]WAVES, Department of Information Technology at Ghent University, Ghent, Belgium
[2]Interuniversity Microelectronics Centre (IMEC), Leuven, Belgium
BioEM 2024, Crete, Greece, June 16-21, 2024

Number of words in the summary: 117 of the 250 allowed.

Number of words in the main text: 2631 of the approximately 2500 allowed.

Summary

Next-generation cellular networks features a higher antenna density and higher frequencies. The hybrid QuaDRiGa/FDTD tool is improved in efficiency and features. In realistic end-to-end simulations, hotspots can appear in an interference pattern of different incident beams. These hotspots are characterized by full width at half-maximum, prominence-to-peak ratio and dimensionality at 28 GHz in a realistic 3D environment with a 6G cell-free massive multiple-input multiple-out network. While there is a high variability across time, the average hotspot features a specific shape. Up to 3 side-lobes are seen around a central peak. Two averaging techniques are proposed and compared: propagation-wise and exposure-wise averaging. The shape of the hotspot in the exposure metric S_{inc} is also examined. Finally, the exposure metrics are plotted as a function of time in a walk through New York City and compared with the ICNIRP guidelines. The exposure metric remain vastly below their limits.

Introduction

The fifth generation (5G) and sixth generation (6G) of cellular networks introduce a higher number of antennas distributed throughout the environment. In a massive multiple-input multiple-output (MaMIMO) 5G transmitter, a large number of antenna elements are collocated and tune their phases and powers to beamform the signal towards the user. In a Distributed or Cell-Free MaMIMO (D-MaMIMO, CF-MaMIMO) 6G network, a large number of Access Points (APs) are distributed throughout the environment and collectively tune their phases and powers to maximize received signal. Radio Stripes (RS) are one implementation of this paradigm [1]. Here, the APs are embedded equidistantly into thin transparent wires fixed to the urban scene. This higher antenna density is required to overcome the increased path loss incurred at higher frequency bands, such as mmWaves (5G) and sub-THz (6G) frequencies.

The International Commission on Non-Ionizing Radiation Protection (ICNIRP) provides guidelines on limits for human Electromagnetic Field (EMF) exposure metrics [2]. Besides *worst-case* simulation studies, *realistic* end-to-end simulations are needed for three reasons. First, to appease unfounded public health concerns [3]. Second, to enable EMF-aware network planning [4]. Third, fully-integrated simulations can characterize wavelength-sized "hotspots": regions of increased EMF shaped by the base station (BS) technology, the propagation environment and the user [4]. The latter is the main focus of this paper.

Two incident plane waves create an interference pattern in the near-field of the UE. In the non-line-of-sight case with a large diversity in angle of arrival, it is generally known that channel precoding forms hotspots. Besides this and their generally spherical nature and a size of several wavelengths, not much is known about these hotspots, especially at mmWave frequencies. This paper reports for the first time detailed characteristics, behavior and visualizations of realistic hotspots at 28 GHz in 3D realistic environments. Moreover, we examine the influence of hotspots on exposure metrics such as the incident power density (S_{inc}) and the new surface absorbed power density (S_{ab}) for frequencies above 6 GHz. This realistic analysis is carried out for a 6-minute walk in New York City (NYC) using an improved state-of-the-art hybrid QuaDRiGa/FDTD tool.

Methods

Improved hybrid QuaDRiGa/FDTD

In 2023, the QUAsi Deterministic RadIo channel GenerAtor (QuaDRiGa) was hybridized for the first time with the Finite-Difference Time-Domain (FDTD) method [4]. Combined with realistic 3D propagation environments, the tool can realistically assess the exposure on humans in end-to-end simulations from 5G and 6G networks. The propagation engine QuaDRiGa and exposure engine Sim4Life are upgraded from versions 2.6 and 6.2 to version 3.1 and 7.2, respectively. QuaDRiGa v3.1 now features GPU and multi-core C++ acceleration. These were leveraged by running the system on a High-Performance Cluster (HPC) with a high core-count and number of GPUs. Sim4Life v7.2 now features the use of *mmWave phantoms*, based on a coated dielectric skin layer. This yields efficiency and accuracy gains, as described in [3]. The tool now supports beamforming to multiple users instead of only one user, paving the way for non-user exposure assessment with e.g., zero-forcing precoding.

When computing the downlink exposure from a CF-MaMIMO 6G system, it was assumed in [4] that every AP holds one antenna. However, these systems likely integrate multiple antenna elements within each AP. This is the case e.g. in RS. Due to the small wavelength at 60 GHz, up to sixteen elements fit within the thin stripes. This paper presents results for a large number of APs of 4x4 patch antennas, distributed in the environment. The crowd-sourced data from OpenCellID provides the locations of real cellular BSs. The hypothetical scenario of a CF-MaMIMO network with APs on these real locations is considered. Although the accuracy is insufficient due to a lack of triangulation data, the antenna density is representative of the digital twin's physical counterpart. Maximum ratio transmission precoding was applied on two users spaced 5 meters apart. As the antenna elements within one AP cannot cooperate with antenna elements from other APs, the precoding is performed in two steps. First, the powers and phases within the 4x4 arrays are tuned to beamform towards the user. Second, the power and phases of all APs are tuned to beamform towards the user. The full CF-MaMIMO system is given a power of 100 W using channel vector normalization. While 100 W is arbitrary, all exposure results are linear w.r.t. this input power.

Hotspot characterization

Two ways to define the location of hotspots are examined. First, exactly where the User Equipment (UE) is located and second, where the fields are highest in a small region around the UE. At this location, three slices are taken through the *x*-, *y*- and *z*-axes. A peak-finding algorithm detects the presence of a hotspot along each axis. The *dimensionality* of a hotspot is the number of axes where a hotspot was found. The Full Width at Half Maximum (FWHM) is the average of all detected FWHMs. The Prominence-to-Peak (P/P) ratio provides a representation of the hotspot's dynamic range, where a ratio of 1 is a peak flanked by fields equaling zero. Finally, two methods are proposed to average exposure metrics across time. The first method is computing the exposure metrics S_{inc} and S_{ab} for each timestep in the walk. The average exposure metrics are then simply the average of all these across time. This is coined *exposure-wise* averaging, because the concept of "exposure at each timestep" is correctly interpreted. The second method is computing the average of the electric and magnetic fields across time first. The average exposure metrics are then S_{inc} and S_{ab} computed for these average EMFs. This is coined *propagation-wise* averaging, because the concept of "average propagated EMFs" is correctly interpreted. Thus, the equations for incident power density are the following:

$$S_{inc,\text{exposure-wise}}(\boldsymbol{r}) = |< \boldsymbol{E}(\boldsymbol{r}) > \times < \boldsymbol{H}(\boldsymbol{r}) >| \ ,$$
$$S_{inc,\text{propagation-wise}}(\boldsymbol{r}) = < |\boldsymbol{E}(\boldsymbol{r}) \times \boldsymbol{H}(\boldsymbol{r})| > \ ,$$

where $< \cdot >$ is the average of a quantity with respect to time. Analogous formulas apply for S_{ab} .

Configuration for realistic exposure along a walk

The scenario shown in Figure 1(a) is considered. After spending 10 seconds indoors, a smartphone user walks from the One World Trade Center (WTC) tower southwards to Liberty Street in NYC, staying indoors for another 10 seconds. The user passes by an open area with foliage, where once WTC 1 and 2 stood before 9/11/2001. Google Earth provides the 3D environment and Google Maps provides the user trajectory. Cellular APs from the neighboring buildings radiate onto the user below tree cover either in Line-Of-Sight (LOS) or Non-Line-Of-Sight (NLOS). The QuaDRiGa channel model distinguishes and interpolates between these in a continuous fashion. The total duration of the walk is 6 minutes. Thus, the 6-minute time-average as defined by ICNIRP can be computed. S_{inc} is the exposure metric used for free-space. For frequencies above 6 GHz and below 30 GHz, S_{ab} averaged over a 4-cm^2 surface is the metric used for exposure on a human. These quantities are plotted along the walk and compared with the ICNIRP limits in Figure 1(b).

Results

Improved hybrid QuaDRiGa/FDTD

Overall, the hybrid QuaDRiGa/FDTD tool is now significantly faster. The propagation part, computed on a 96-core HPC achieves a 90-fold increase in speed. The hybridization part, computing only values on the sides of Huygens box, achieves a 16-fold increase. The exposure part, modeling the absorbed fields in the skin efficiently, achieves a 64-fold increase. Together, this paves the way for sub-THz exposure assessment and the comparison of exposure in different cities, countries and environments.

The receiver separation is defined as the average difference in signal gain between the two users walking 5 meters from each other. Only the first user's UE is focused. Hence, a high receiver separation indicates functioning precoding. When only the antenna elements within each AP are precoded, the receiver separation increases by 6.01 dB along the walk. All APs beamform towards the user, but the nearest APs do not necessarily emit most power. When only the APs themselves are precoded, the receiver separation increases by 4.74 dB. None of the APs beamform towards the user, but the nearest APs emit most power. When both precodings are combined, the receiver separation is 10.08 dB. The exposure metrics as a result of this signal are considered in the following.

Hotspot characteristics

Within a large-scale region exposed by the beams, hotspots can increase the aforementioned 10.08 dB gain locally, at or within several wavelengths of the receiver. A free-space domain of 5.1 x 4.1 x 7.1 cm is considered, fitting a human ear, with a resolution of 10 cells per wavelength. The mean and standard deviation were computed based on 316 timesteps along the walk. These results are shown in Table 1.

Table 1: A comparison of hotspot characteristics when defined to be at the receiver or at the point with the highest field near the receiver. The mean and standard deviation are given based on the S_{inc} metric.

	At the receiver	**At highest field**
Distance from center [cm]	0.0	2.82 ± 1.09
Peak [W]	2.06e-10 ± 8.77e-10	4.08e-10 ± 1.65e-9
FWHM [cm]	1.13 ± 0.45	0.94 ± 0.38
P/P ratio [%]	63 ± 26	57 ± 25
Dimensionality equals 3 [%]	84.5	96.2

The means of the FWHM and P/P ratio indicate a size in the order of one wavelength (1.07 cm) and a clearly pronounced peak, respectively. The distance from the center for the point with the highest field is 2.82 cm on average, about 30% of the domain's diagonal. However, the density of hotspots per cm^3

is highest in the center. Over 50% of hotspots are within 0.3 cm of the center, with many outliers. The standard deviations of the FWHM and P/P ratio are high, approximately 40% of their mean. When viewing a movie of the field distribution along the walk, the hotspot's location and shape changes frequently, but in a continuous fashion due to the time-continuity of the propagation engine. During 96% of the walk, the dimensionality equals 3, indicating a roughly ellipsoidal or spherical shape. The hotspots vanish or are reduced to a simple interference pattern when one or two strong LOS components are present, respectively. They also vanish when no precoding is applied.

Shape and visualization of an average hotspot

At any specific timestep, a hotspot can appear in a variety of shapes, sizes and locations. However, a characteristic shape appears when the hotspot is averaged in time. ICNIRP also specifies that exposure metrics should be averaged over 6-minute intervals. Figure 2(a) depicts a horizontal slice through the receiver, positioned in the center. The complex norm of the electric field is shown because it is a component in the formula for propagation-wise S_{inc}. The main peak is located in the center with a FWHM of 0.47 cm. The peak is flanked by troughs at 25% of its value, yielding a 75% P/P ratio (90% with the deepest troughs). A first-order side-lobe is observed at 0.61 λ with a peak value equaling 50% of the main peak. A second-order side-lobe is observed at 1.15 λ. Angular dependence is observed in the 2D slice, showing peaks and troughs for certain azimuthal angles. Figure 2(b) shows the radial probability density function of the field with respect to distance. For a certain distance $r \pm dr$, the field values are collected in a distribution. The graph displays the 25^{th}, 50^{th} and 75^{th} percentile of this distribution as a function of r with dr equaling 0.15 mm. The same main, first- and second-order side-lobes are observed. A faint third-order is observed at 1.76 λ. As the distance approaches the edges of the domain, a constant field remains, which is 25% of the peak in the main lobe. Therefore, the small-scale hotspot increases the electric field by 12 dB on top of the large-scale beamforming gain. A higher number of antenna elements and APs increases this gain, in theory without bounds [5]. More research is needed to assess the exposure of extremely massive MIMO systems. Within each side-lobe, peaks and troughs appear as a function of the azimuthal and elevation angles. The internal structure of a hotspot can be loosely compared to the probability density function of electrons around an atom with several valence bands.

The magnetic field of the hotspot behaves analogously to a typical interference pattern: when the electric field phasor reaches a peak in space, the magnetic field reaches a trough, and vice-versa. Figure 3(a) shows S_{inc} for the 2D slice. The expression for S_{inc} combines the electric and magnetic fields. The hotspot also combines the features of the electric and magnetic field hotspots. The small peak at the center is the combination of an electric-field peak and a magnetic-field trough. This is flanked by higher peaks originating from the first-order magnetic-field side-lobes. The side-lobe series continues with alternating peaks from both fields.

With propagation-wise averaging, positive EMFs at one timestep can cancel out negative EMFs at another timestep. However, from an exposure assessment point-of-view, both positive and negative field values can contribute to dielectric heating. The exposure-wise average of S_{inc} is visualized in Figure 3(b) in the same 2D slice. A more chaotic interference pattern is seen with its highest peak not at the center. The FWHM is 0.99 cm and the P/P ratio is 37% with the deepest troughs. The pattern is overlaid on a constant envelope. This causes the first-order troughs to be 2.5 times less deep than with propagation-wise averaging.

Realistic exposure along a walk

Figure 1(b) shows the exposure metrics S_{inc} and S_{ab} along the walk on the left vertical axis. The maximal S_{inc} is compared with the median S_{inc} in the domain to illustrate the hotspot gain. The fully precoded case is compared with the fully unprecoded case. The exposure is constant when the user is indoor. The exposure is time-continuous and consistent with the environment, e.g., the signal increases substantially when near APs and when the user is in LOS. The maximal exposure metric for S_{inc} is -78.8 dBW for a

100 W total power in the CF-MaMIMO network. For S_{ab}, it is -92.8 dBW. The ratio of the exposure metric divided by the relevant ICNIRP exposure limit is shown on the right vertical axis.

Conclusions

The hybrid QuaDRiGa/FDTD tool was improved through a 90, 16 and 64-fold increase in speed in the propagation, hybridization and exposure steps. Multi-user MIMO is now possible, and we show that receiver signal separation increases with precoding a CF-MaMIMO network by 10.08 dB. The hotspots from a walk in NYC were characterized by FWHM, P/P ratio and dimensionality. While there is a high variability across time, the average hotspot features a specific shape, proposing propagation-wise and exposure-wise averaging. Up to 3 side-lobes are seen around a central peak. The shape of the hotspot in the exposure metric S_{inc} is also examined. Finally, the exposure metrics are plotted as a function of time in a walk through NYC.

Acknowledgements

This work was supported by the ERC through “ATTO: A New Concept for Ultrahigh Capacity Wireless Networks” under Grant 695495 and Methusalem through “SHAPE: Next Generation Wireless Networks”.

References

[1] Z. H. Shaik, E. Björnson and E. G. Larsson, "Cell-Free Massive MIMO with Radio Stripes and Sequential Uplink Processing," 2020 IEEE International Conference on Communications Workshops (ICC Workshops), Dublin, Ireland, 2020, pp. 1-6.

[2] ICNIRP, “Guidelines for limiting exposure to electromagnetic fields (100 kHz to 300 GHz)”, Health Phys, 118(00):000–000, 2020.

[3] R. Wydaeghe et al., “Accelerating mmWave exposure simulations and the OUTREACH idea to industry,” in Third International Conference on Bioelectromagnetics, Crete, Greece, unpublished.

[4] R. Wydaeghe et al., “New Hybrid QuaDRiGa-FDTD Method for Realistic Human Exposure Assessment at 28 GHz with 6G Cell-Free Massive MIMO in 3D Outdoor Environments,” in Second International Conference on Bioelectromagnetics, Oxford, England, Jun. 2023.

[5] J. Hoydis, S. ten Brink and M. Debbah, "Massive MIMO: How many antennas do we need?," 2011 49th Annual Allerton Conference on Communication, Control, and Computing (Allerton), Monticello, IL, USA, 2011, pp. 545-550.

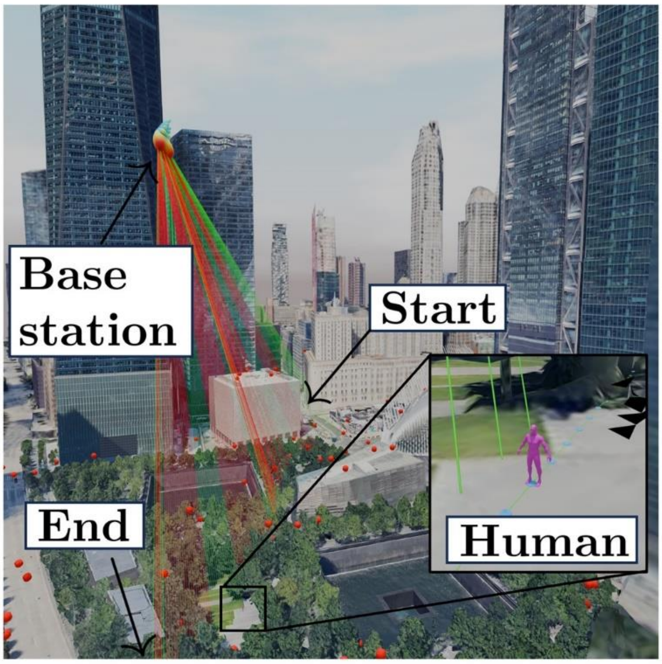

(a) The environment of the walk

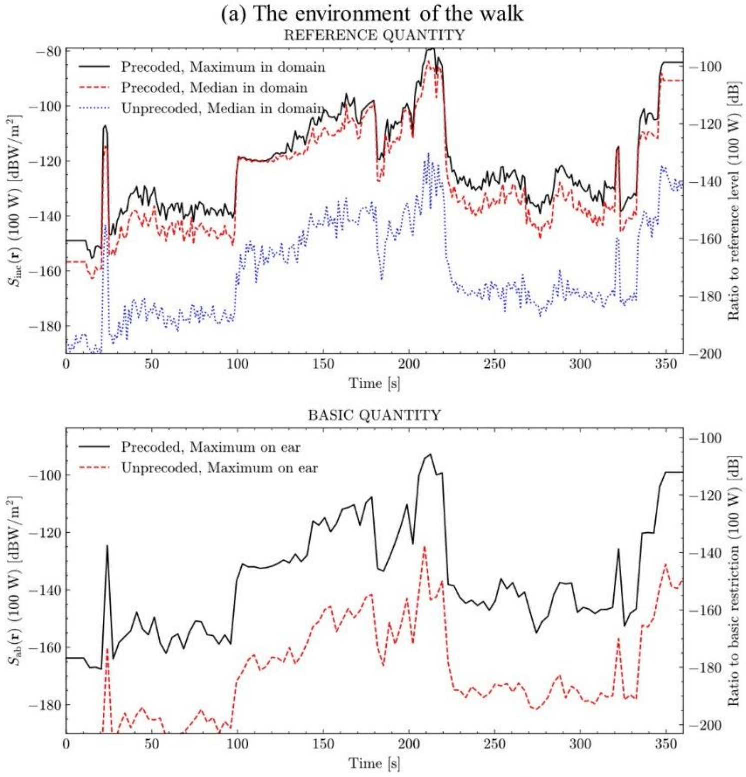

(a) The exposure along the walk

Figure 1: Top: a walk (blue dots) in the WTC of NYC is shown with the APs of a CF-MaMIMO system (red dots) and one the LOS/NLOS distinction from one AP (lines). 3D realistic buildings are used with a frequency at 28 GHz. Bottom: the reference (S_{inc}) and basic (S_{ab}) exposure quantities are plotted along the walk. The right axis shows the ratio w.r.t. the ICNIRP limits. The influence of the hotspot is shown in free-space.

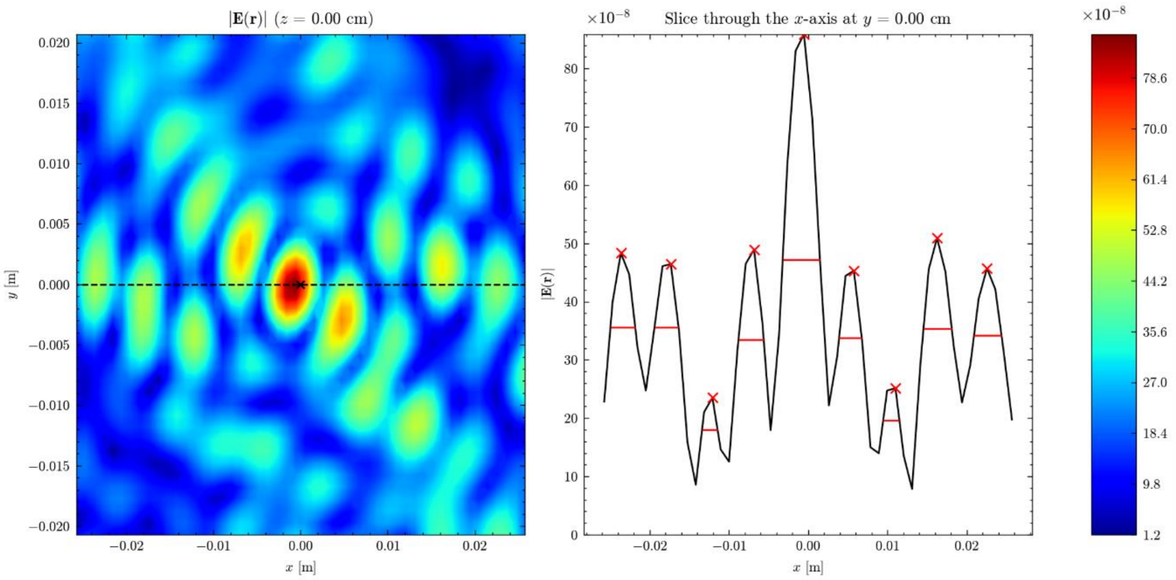

(a) Visualization of the hotspot

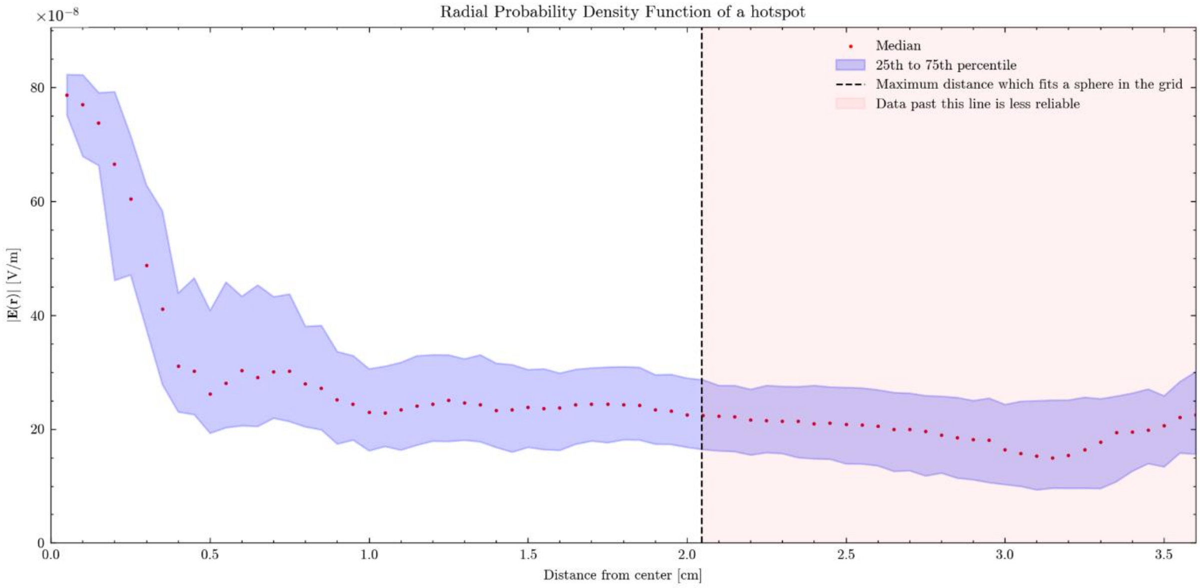

(a) Radial distribution of a hotspot

Figure 2: Visualization of a hotspot's electric field when averaged propagation-wise. Top: a 2D and 1D slice through the focused UE. Bottom: the radial probability density function of the fields, showing the 25^{th}, 50^{th} and 75^{th} percentiles of all fields at a certain distance (± 0.15 mm).

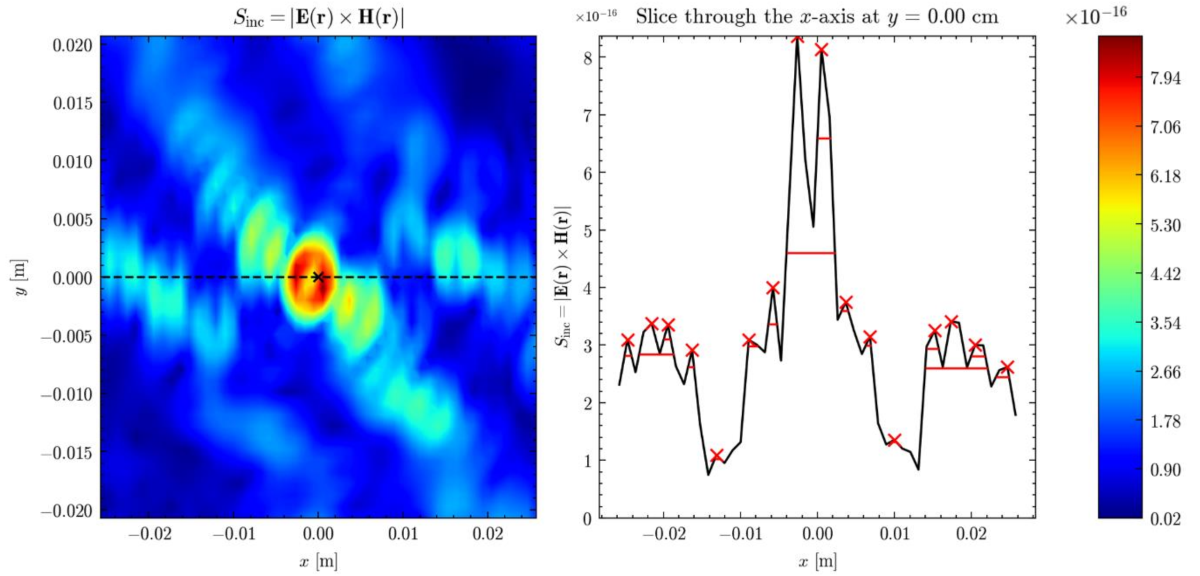

(a) Propagation-wise average of the hotspot

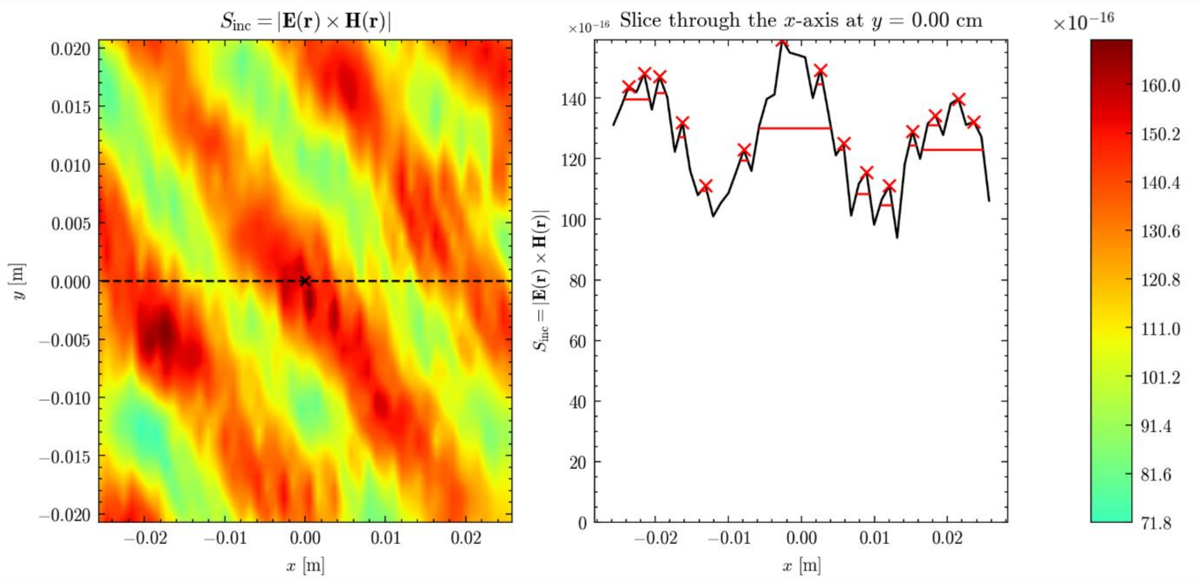

(b) Exposure-wise average of the hotspot

Figure 3: Comparison of the S_{inc} with the propagation- and exposure-wise averaging using 2D and 1D slices. The former averages the fields in time first, the latter computes the exposure first and then averages these in time.